

# Redshift space bias and $\beta$ from the halo model

Uroš Seljak

Department of Physics, Jadwin Hall  
Princeton University, Princeton, NJ 08544

August 2000

## ABSTRACT

We analyze scale dependence of redshift space bias  $b$  and  $\beta \equiv \Omega_m^{0.6}/b$  in the context of the halo model. We show that linear bias is a good approximation only on large scales, for  $k < 0.1h\text{Mpc}^{-1}$ . On intermediate scales the virial motions of galaxies cause a suppression of the power spectrum relative to the linear one and the suppression differs from the same effect in dark matter. This can potentially mimic the effect of massive neutrinos and the degeneracy can only be broken if power spectrum is measured for  $k \ll 0.1h\text{Mpc}^{-1}$ . Different methods to determine  $\beta$  converge for  $k < 0.1h\text{Mpc}^{-1}$ , but give drastically different results on smaller scales, which explains some of the trends observed in the real data. We also assess the level of stochasticity by calculating the cross-correlation coefficient between the reconstructed velocity field divergence and the galaxies and show that the two fields decorrelate for  $k > 0.1h\text{Mpc}^{-1}$ . Most problematic are galaxies predominantly found in groups and clusters, such as red or elliptical galaxies, where we find poor convergence to a constant bias or  $\beta$  even on large scales.

## 1 INTRODUCTION

Determination of the power spectrum of mass fluctuations is one of the main goals of existing and upcoming galaxy surveys. Current state of the art is PSCz (Saunders et al. 2000), which has a near spherical geometry and consists of about 15000 measured galaxy redshifts. Upcoming surveys, such as 2dF\* and SDSS †, will measure redshifts of up to a million galaxies. 3-dimensional mass power spectrum is sensitive to a number of cosmological parameters, such as the matter and baryon density, shape and amplitude of initial fluctuations and the Hubble constant. This sensitivity is further improved if additional information from cosmic microwave background (CMB) anisotropies is included (Eisenstein, Hu & Tegmark 1999). Mass power spectrum is particularly important for determination of neutrino mass. Massive neutrinos have only a minor impact on the CMB, but they strongly suppress the level of mass fluctuations on small scales because of the high neutrino momentum before they become nonrelativistic. In principle the sensitivity of upcoming surveys is such that it will be possible to test neutrino masses below 0.1-1eV (Hu, Eisenstein & Tegmark 1998), close to those suggested by recent Super-Kamiokande neutrino results (Fukuda et al. 1998). A possible concern is that the effect of massive neutrinos becomes important on small scales, where the assumption of galaxies tracing dark matter may not hold. One of the purposes of this paper is to investigate how serious this problem is and, more generally, what is the

relation between the observed redshift space galaxy power spectrum and the underlying linear dark matter spectrum.

The relation between the galaxies and the dark matter clustering has recently been analyzed in the context of the halo model (Seljak 2000; Peacock & Smith 2000; Scoccimarro et al. 2000). In this model all the mass in the universe is divided up into halos of different mass. These halos cluster according to the linear theory, up to an overall amplitude which depends on the halo mass (halo biasing). To these correlations important on large scales one adds correlations on small scales, which arise from within the same halos. For the latter one needs to specify the radial halo profile, which can also be a function of halo mass. This approach has been successful in reproducing the nonlinear dark matter power spectrum and its transition to the linear regime (Seljak 2000; Scoccimarro et al. 2000; Ma & Fry 2000).

Galaxies differ from the dark matter in their galaxy multiplicity function, which parametrizes the number of galaxies inside the halo as a function of halo mass. For a magnitude limited sample this function is zero for low mass halos which cannot host bright  $L_*$  galaxies, which already implies that galaxies cannot trace dark matter exactly. Above the threshold the number of galaxies increases with the halo mass, but need not grow linearly, as suggested by the gas cooling arguments where gas in more massive and thus hotter halos takes longer to cool and form stars. In addition to the multiplicity function there is another effect that changes the galaxy clustering properties: one galaxy is expected to form at the halo center, which enhances the correlations on small scales. These features naturally explain many of the observational properties of galaxy clustering in real space, such as the power law growth on small scales and the delayed on-

\* <http://meteor.anu.edu.au/colless/2dF>

† <http://www.astro.princeton.edu/BBOOK>

set of nonlinear clustering in the translinear regime (Seljak 2000; Scoccimarro et al. 2000; Peacock & Smith 2000).

Previous work in the halo model has focused on the clustering in real space, while most of existing and upcoming surveys operate in redshift space. Redshift space distortions enhance the correlations on large linear scales and suppress them on small scales. This changes the clustering pattern in a nontrivial way and it is therefore important to include these effects when studying the relation between the galaxy and the dark matter power spectrum. As an added bonus, redshift distortions also allow one to determine  $\beta = \Omega_m^{0.6}/b$ , where  $\Omega_m$  is the mass density and  $b$  the bias parameter of the galaxies. There are several existing methods to determine this parameter in the literature (see (Strauss & Willick 1995) for a review). In this paper we address whether different methods to determine  $\beta$  converge and what is the survey size needed for this.

## 2 THE HALO MODEL

The halo model uses the Press-Schechter (Press & Schechter 1974) picture for dark matter, which assumes all the matter is in a form of isolated halos with a well defined mass  $M$  and halo profile  $\rho(r, M)$ , which can be modelled as

$$\rho(r) = \frac{\rho_s}{(r/r_s)^{-\alpha}(1+r/r_s)^{3+\alpha}}, \quad (1)$$

where N-body simulations give  $1 < \alpha < 1.5$  (Navarro, Frenk & White 1996; Moore et al. 1998). For the power spectrum analysis adopted here it is convenient to introduce the Fourier transform of the halo profile, normalized to unity on large scales,

$$y(k) = \frac{1}{M} \int \rho(r) \frac{\sin(kr)}{kr} d^3r. \quad (2)$$

The mass is determined by the total mass within the virial radius  $r_v$ , defined to be the radius where the mean density within it is  $\delta_{\text{vir}} = 200$  times the mean density of the universe. The concentration parameter  $c = r_v/r_s$  in general depends on the halo mass. In this paper we will use  $\alpha = 1.5$  and  $c(M) = 6(M/M_*)^{-0.15}$ , where  $M_*$  is the nonlinear mass scale defined below. This choice fits well the results of N-body simulations (Moore et al. 1998) and has been shown to give good agreement with real space power spectra from N-body simulations (Seljak 2000), but we note that other fits with  $\alpha = 1$  and a different choice of  $c(M)$  can give equally good agreement with these.

In the halo model the power spectrum consists of two terms. The first is that due to a system of correlated halos, with inter-halo correlations assumed to be a biased sampling of  $P_{\text{lin}}(k)$ . Since the real space convolution is simply a Fourier space multiplication this contribution is

$$P^{hh}(k) = P_{\text{lin}}(k) \left[ \int f(\nu) d\nu b(\nu) y(k; M) \right]^2 \quad (3)$$

where  $b(\nu)$  is the (linear) bias of a halo of mass  $M(\nu)$  and  $f(\nu)$  is the multiplicity function. The peak height  $\nu$  is related to the mass of the halo through

$$\nu \equiv \left( \frac{\delta_c}{\sigma(M)} \right)^2 \quad (4)$$

where  $\delta_c = 1.69$  and  $\sigma(M)$  is the rms fluctuation in the matter density smoothed with a top-hat filter on a scale  $R = (3M/4\pi\bar{\rho})^{1/3}$ . We use (Sheth & Tormen 1999)

$$b(\nu) = 1 + \frac{\nu - 1}{\delta_c} + \frac{2p}{\delta_c(1 + \nu'^p)} \quad (5)$$

and

$$\nu f(\nu) = A(1 + \nu'^{-p})\nu'^{1/2}e^{-\nu'/2} \quad (6)$$

where  $p = 0.3$  and  $\nu' = 0.707\nu$ . The normalization constant  $A$  is fixed by the requirement that all of the mass lie in a given halo

$$\int f(\nu) d\nu = 1. \quad (7)$$

On small scales pairs lying within a single halo become dominant

$$P^P(k) = \frac{1}{(2\pi)^3} \int f(\nu) d\nu \frac{M(\nu)}{\bar{\rho}} |y(k)|^2. \quad (8)$$

The total power spectrum is the sum of the two contributions,

$$P_{\text{dm}}(k) = P_{\text{dm}}^{hh}(k) + P_{\text{dm}}^P(k). \quad (9)$$

For galaxies the above model needs to be modified in several aspects. Instead of the dark matter particles we are now counting galaxies inside halos. Small halos cannot host very bright galaxies, so there is a lower mass cutoff in the halo distribution at a given luminosity cutoff. In addition, number of galaxies inside halo need not grow linearly as a function of halo mass. Both of these features can be accounted for by introducing two galaxy multiplicity functions,  $\langle N \rangle(M)$  and  $\langle N(N-1) \rangle^{1/2}(M)$ , which count mean number of galaxies inside the halo both linearly and pair weighted, respectively. Second modification is that radial profile of galaxy distribution,  $y_g(k)$ , need not be the same as that of the dark matter  $y(k)$ . Both observations (Carlberg et al. 2000) and numerical simulations (Diaferio et al. 1999) show that at least for some types of galaxies the two functions must differ. Here we will for the most part adopt the approach where the two are equal, but we also discuss the modifications when this assumption is dropped. Finally, one expects there will be one galaxy which forms at the center of the halo. The correlations between this galaxy and the rest of the galaxies inside the halo will be sensitive only to a single convolution in the radial profile. For large halos with  $\langle N(N-1) \rangle^{1/2} \gg 1$  the presence of the central galaxy does not change significantly the number of pairs or their statistics. For small halos where  $\langle N(N-1) \rangle^{1/2} \ll 1$  its existence changes the correlations significantly and is in fact necessary to explain the steep power law in the galaxy correlation function to small scales (Seljak 2000; Peacock & Smith 2000).

Putting the above together we have,

$$P_{\text{gg}}^{hh}(k) = P_{\text{lin}}(k) \left[ \frac{\bar{\rho}}{\bar{n}} \int f(\nu) d\nu \frac{\langle N \rangle}{M} b(\nu) y(k, M) \right]^2, \quad (10)$$

where  $\bar{n}$  is the mean density of galaxies in the sample,

$$\int \frac{\langle N \rangle}{M} f(\nu) d\nu = \frac{\bar{n}}{\bar{\rho}}. \quad (11)$$

The Poisson term is given by

$$P_{\text{dm}}^P(k) = \frac{1}{(2\pi)^3 \bar{n}^2} \int \frac{M}{\bar{\rho}} f(\nu) d\nu \frac{\langle N(N-1) \rangle}{M^2} |y(k, M)|^p, \quad (12)$$

where we approximate the effect of the central galaxy by using  $p = 1$  for  $\langle N(N-1) \rangle < 1$  and  $p = 2$  otherwise.

In redshift space there are two effects which modify the above expressions. The first is a boost of power on large scales due to streaming of matter into overdense regions (Kaiser 1987). The second is a reduction of power on small scales due to virial motions within an object (Peacock & Dodds 1994). In the halo model these two effects can be separated into the halo-halo and one halo (Poisson) contributions. In this model the virial motion suppression becomes a function of scale, since larger halos (with larger velocity dispersions) dominate at larger scales than smaller halos. In contrast to the previous models (Hatton & Cole 1999) this model successfully reproduces N-body simulation results (White 2000).

In linear theory a density perturbation  $\delta_k$  generates a velocity perturbation  $\dot{\delta} = -ikv$  with  $\vec{v}$  parallel to  $\vec{k}$ . Using the plane-parallel approximation ( $kr \gg 1$ ) the redshift space galaxy density perturbation  $\delta_g^{\text{rs}}$  is given by

$$\delta_g^{\text{rs}} = \delta_g + \delta_v \mu^2, \quad (13)$$

where  $\mu = \hat{r} \cdot \hat{k}$ ,  $\delta_g$  is the real space galaxy density perturbation and  $\delta_v$  is the velocity divergence. This can be related to the density perturbation  $\delta_{\text{dm}}$  via  $\delta_v = f\delta_{\text{dm}}$ , where  $f(\Omega) \equiv d \log \delta / d \log a \simeq \Omega_m^{0.6}$  and  $a$  is the scale-factor.

On small scales virial motions within collapsed objects act as a gaussian convolution in redshift space, which suppresses power. We will model this as a gaussian filter with mass dependent 1-d velocity dispersion  $\sigma$ , acting on the mode component along the line of sight. Assuming that the halos are isothermal we may use the mass within the virial radius to obtain the 1D velocity dispersion of a halo of mass  $M$ ,

$$\sigma = [GM/2r_{\text{vir}}]^{1/2} \sim 7H_0 r_{\text{vir}}, \quad (14)$$

where  $H_0$  is the Hubble constant and  $r_{\text{vir}}$  is the virial radius, which can be related to the halo virial mass,  $M_{\text{vir}} = 4\pi \delta_{\text{vir}} \bar{\rho} r_{\text{vir}}^3 / 3$ . The density contrast in redshift space is

$$\delta_g^{\text{rs}} = \delta_g e^{-(k\sigma\mu)^2/2}. \quad (15)$$

Since the power spectrum is in general a function of both  $k$  and  $\mu$  we must decide which quantity we are interested in before proceeding. The most common is to average over  $\mu$  to obtain the isotropized power spectrum. On large scales this implies averaging over  $\mu$  the square of equation 13. This can be further improved by including the small scale dispersion, obtained by radially averaging equation 15. On small scales we only need to average over the square of equation 15, since there is no linear effect.

Combining the above the isotropized redshift space power spectrum in the halo model becomes

$$P_0(k) = \left( F_g^2 + \frac{2}{3} F_v F_g + \frac{1}{5} F_v^2 \right) P_{\text{lin}}(k) + \frac{1}{(2\pi)^3 \bar{n}^2} \int \frac{M}{\bar{\rho}} f(\nu) d\nu \frac{\langle N(N-1) \rangle}{M^2} \mathcal{R}_p(k\sigma) |y_g(k, M)|^p, \quad (16)$$

where

$$F_v = f \int f(\nu) d\nu b(\nu) \mathcal{R}_1(k\sigma) y(k, M)$$

$$F_g = \frac{\bar{\rho}}{\bar{n}} \int f(\nu) d\nu \frac{\langle N \rangle(M)}{M} b(\nu) \mathcal{R}_1(k\sigma) y_g(k, M) \quad (17)$$

and

$$\mathcal{R}_p(\alpha = k\sigma[p/2]^{1/2}) = \frac{\sqrt{\pi}}{2} \frac{\text{erf}(\alpha)}{\alpha}, \quad (18)$$

for  $p = 1, 2$ .

Figure 1 shows various bias functions as a function of  $k$ , defined as the square root of the ratio of the galaxy to the linear dark matter power spectrum. Throughout we use  $\Lambda CDM$  model with  $\Omega_m = 0.3$ ,  $\Omega_\lambda = 0.7$ , normalized to  $\sigma_8 = 0.9$  today. Linear dark matter power spectrum is used here, since this is the quantity we wish to reproduce. Also shown is the square root ratio of the nonlinear redshift space dark matter spectrum to the linear power spectrum. This quantity can be compared directly to the N-body simulations and we verified it is in remarkable agreement with those (see also White 2000). It is interesting to note that the redshift space dark matter power spectrum agrees to within 10% with the real space linear power spectrum over the entire range of scale. This is somewhat coincidental, since for the nonlinear redshift space power spectrum the correlated halo-halo term is suppressed on small scales because of virial motions ( $\mathcal{R}_1(k\sigma) < 1$ ) and because of halo profile ( $y(k, M) < 1$ ). The difference is picked up by the Poisson term, which does not depend on the linear power spectrum at all (except through the mass dependence of the concentration parameter).

For galaxies we see that the linear bias, defined as the ratio of the redshift space galaxy power spectrum to the linear dark matter spectrum, typically exceeds the redshift space dark matter bias on large scales. This is of course not surprising and reflects the fact that galaxies are a biased tracer of dark matter. For galaxies found predominantly in groups and clusters the bias is larger than for those which are also found in the field. The choice of the galaxy multiplicity function used here is motivated by the semi-analytic models of galaxy formation (Benson et al. 2000; Kauffmann et al. 1999). Least biased are regular galaxies selected only on the basis of their luminosity (dashed line). More biased are red galaxies with  $M_B - M_V > 0.8$  in semi-analytic models of Kauffmann et al. (1999; dash-dotted), while most biased are those with  $M_B - M_V > 2$  (dotted). It is important to emphasize that these are just plausible choices of the galaxy multiplicity function as the data at present do not allow one to determine these directly. Theoretical models of galaxy multiplicity function can vary at least at the level of 30%, leading to variations of up to 150 km/s in 1-d velocity dispersion. For this reason we only emphasize the features of the model which are generic and expected for any choice of the parameters, even though the relative importance of different effects may vary from model to model. For example, in all cases the galaxy multiplicity function is expected to increase less rapidly with the halo mass than the mass itself, but may have a different low mass cutoff and/or different shape.

The bias is scale independent on large scales for the regular galaxies. For these bias becomes scale dependent above  $k > 0.1h\text{Mpc}^{-1}$ , on scale somewhat smaller than for the dark matter. This is because these galaxies are preferentially found in smaller halos relative to the dark matter, and are hence dominated by systems with smaller  $\sigma$ , thus the virial

motion suppression is smaller. Just as in the case of the dark matter the galaxy linear bias first declines with scale. This is because correlations are suppressed both by the finite extent of the halos and by the virial motions within them. At even smaller scales, above  $k > 1h\text{Mpc}^{-1}$ , bias begins to rise again. This is caused by the nonlinear Poisson term for the galaxies, not present in the linear power spectrum, which enhances the correlations on small scales. This is of course the term that gives rise to the nonlinear clustering pattern and the familiar power law slope. Just as in the real space in the redshift space the enhancement is also more important for the galaxies than for the dark matter. One reason for this is that galaxies are preferentially found in smaller systems relative to the dark matter, so the suppression because of finite halo extent and virial motions is less important than for the dark matter. Another is that on smaller scales the correlations are dominated by small halos with  $\langle N \rangle < 1$ . In these there is a central galaxy, which does not contribute to the suppression because of halo profile and virial motions, leading to an enhancement of the galaxy power spectrum over that of the dark matter. Finally, a more concentrated distribution of galaxies relative to the dark matter, as suggested by some observations (Carlberg et al. 2000), would also lead to an enhancement of the galaxy power spectrum relative to that of the dark matter.

The choices motivated by red or elliptical galaxies in semi-analytic models (Kauffmann et al. 1999) eliminate galaxies in less massive halos. These are shown in figure 1 as the dash-dotted and dotted lines, for the case of red ( $M_B - M_V > 0.8$ ) and very red ( $M_B - M_V > 2$ ) galaxies, respectively. The bias in this case shows scale dependence even on very large scales,  $k < 0.01h\text{Mpc}^{-1}$ . This is because the Poisson term becomes important again relative to the linear power spectrum on very large scales, where the latter approaches slope  $n \sim -1$ , while the former remains at  $n = 0$ . Galaxies that are only found in rarer, more massive, systems have the Poisson term that is larger, so this effect is relatively more important for this type of galaxies as opposed to the normal galaxies. For the same reason that these galaxies are in more massive halos the virial motion and finite halo size suppression become important on larger scales and the bias is already scale dependent for  $k \sim 0.1h\text{Mpc}^{-1}$ . On smaller scales the bias dependence is also sensitive to whether the galaxies are central inside the halo or not and whether the radial distribution follows that of dark matter, both of which can have important impact on the bias. For example, if red galaxies avoid centers of halos (because the gas preferentially cools to the halo center, where it can form new stars which are blue), then the bias is a less rapidly rising function of  $k$  on small scales than that shown in figure 1).

### 3 $\beta$ FROM REDSHIFT DISTORTIONS

Another application of the redshift distortion analysis is to extract the parameter  $\beta = f/b$ . There are many different ways to do this (see Strauss & Willick 1995 for a review). The two examples used here are by combining the galaxy power spectrum  $P_{gg}$  with the velocity power spectrum  $P_{vv}$  or their cross-spectrum  $P_{vg}$  and by using Legendre expansion of redshift space power spectrum. If bias is constant on large

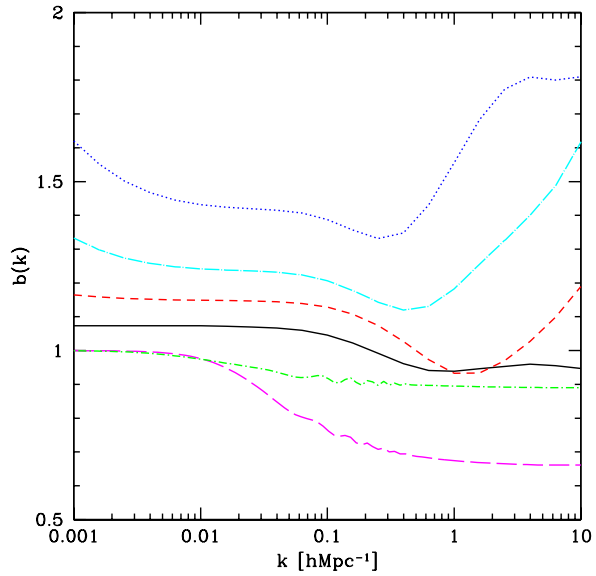


**Figure 1.** Bias  $b(k)$  defined as the square root of the ratio of redshift space nonlinear power spectrum to the linear dark matter spectrum. From top to bottom are shown very red galaxies ( $M_B - M_V > 2$ , dotted), red galaxies ( $M_B - M_V > 0.8$ , long dash-sotted), normal galaxies (short dashed) and dark matter (solid). The bottom two lines are ratios between massive and massless neutrino transfer functions, for  $m_\nu = 0.1\text{eV}$  (upper, short dash-dotted) and  $m_\nu = 1\text{eV}$  (lower, long-dashed).

scales  $\beta$  will also be a constant, but in the more general case considered here it will be scale dependent. Moreover, different methods may not even agree on a given scale, so the meaning of  $\beta$  itself becomes questionable.

Given that in general the power spectrum is a function of both  $\mu$  and  $k$  it is not possible to extract the three components  $P_{gg}$ ,  $P_{vg}$  and  $P_{vv}$  from it uniquely, since it depends on the adopted procedure. In fact, a clean separation into the three components is only possible on large scales where only the linear compression redshift distortion operates. To obtain an idea what happens when small scale effects become important we perform angular averages assuming linear theory model and reconstruct the 3 components from these. As before we assume plane-parallel approximation. For isotropic averaging in equation 17 this gives

$$P_0(k) = \frac{1}{2} \int_{-1}^{+1} d\mu \ (\delta_g + \mu^2 \delta_v)^2 = P_{gg} + \frac{2}{3} P_{vg} + \frac{1}{5} P_{vv}. \quad (19)$$

Similarly we can also perform averaging with  $\mu^2$  and  $\mu^4$  weights,

$$P_2(k) = \frac{1}{2} \int_{-1}^{+1} \mu^2 d\mu \ (\delta_g + \mu^2 \delta_v)^2 = \frac{1}{3} P_{gg} + \frac{2}{5} P_{vg} + \frac{1}{7} P_{vv}$$

$$P_4(k) = \frac{1}{2} \int_{-1}^{+1} \mu^4 d\mu \ (\delta_g + \mu^2 \delta_v)^2 = \frac{1}{5} P_{gg} + \frac{2}{7} P_{vg} + \frac{1}{9} P_{vv}. \quad (20)$$

From  $P_0$ ,  $P_2$  and  $P_4$  we can reconstruct uniquely  $P_{gg}$ ,  $P_{vg}$  and  $P_{vv}$  using the above expressions. At the same time the halo model also gives predictions for the averaged spectra

$P_2$  and  $P_4$  just like for  $P_0$  (equation 17). These are given by

$$\begin{aligned} P_2(k) &= \left( \frac{1}{3} F_g^2 + \frac{2}{5} F_v F_g + \frac{1}{7} F_v^2 \right) P_{\text{lin}}(k) \\ &+ \frac{1}{(2\pi)^3 n^2} \int \frac{M}{\rho} f(\nu) d\nu \frac{\langle N(N-1) \rangle}{M^2} \mathcal{R}_{p+2}(k\sigma) |y_g(k, M)|^p \\ P_4(k) &= \left( \frac{1}{5} F_g^2 + \frac{2}{7} F_v F_g + \frac{1}{9} F_v^2 \right) P_{\text{lin}}(k) \\ &+ \frac{1}{(2\pi)^3 n^2} \int \frac{M}{\rho} f(\nu) d\nu \frac{\langle N(N-1) \rangle}{M^2} \mathcal{R}_{p+4}(k\sigma) |y_g(k, M)|^p, \end{aligned} \quad (21)$$

where

$$\mathcal{R}_{p+q}(k\sigma) = \int_0^1 \mu^q e^{-p(k\sigma\mu)^2/2} d\mu, \quad (22)$$

which have simple analytic expressions similar to equation 18,

$$\mathcal{R}_{p+2}(\alpha = k\sigma[p/2]^{1/2}) = \frac{\sqrt{\pi}}{4} \left[ \frac{\text{erf}(\alpha)}{\alpha^3} - \frac{e^{-\alpha^2}}{2\alpha^2} \right] \quad (23)$$

$$\mathcal{R}_{p+4}(\alpha = k\sigma[p/2]^{1/2}) = \frac{3\sqrt{\pi}}{8} \left[ \frac{\text{erf}(\alpha)}{\alpha^5} - \frac{e^{-\alpha^2}}{2\alpha^2} \left( 1 + \frac{3}{2\alpha^2} \right) \right],$$

for  $p = 1, 2$ .

The procedure to extract  $\beta$  is the following: first we compute  $P_0$ ,  $P_2$  and  $P_4$  from above expressions. Next we assume they are determined by the linear combinations of  $P_{\text{gg}}$ ,  $P_{\text{vg}}$  and  $P_{\text{vv}}$  as valid in linear theory, which allows one to determine them uniquely. We then take ratios  $[P_{\text{vv}}/P_{\text{gg}}]^{1/2}$  and  $P_{\text{vg}}/P_{\text{gg}}$  to determine  $\beta$ . These results are shown in figure 2 for normal (top) and red ( $M_B - M_V > 0.8$ ; bottom) galaxy sample used in figure 1. We see that for normal galaxies the two reconstructed  $\beta$  functions are approximately constant and equal for  $k < 0.1h\text{Mpc}^{-1}$ . For  $k > 0.1h\text{Mpc}^{-1}$  the two  $\beta$  functions diverge away from the large scale value and away from each other. This indicates that on scales below  $50h^{-1}\text{Mpc}$  one cannot extract the true value of  $\beta$  and that different methods of determining it can give rather different answers. This is because on these scales virial motions within halos become important and pure linear theory ansatz is no longer valid. The scale dependence of the two  $\beta$  reconstructions is in qualitatively good agreement with the behaviour seen in real data. For example, (Hamilton, Tegmark & Padmanabhan 2000) have decomposed the data in a similar way to  $P_{\text{gg}}$ ,  $P_{\text{vg}}$  and  $P_{\text{vv}}$ . Their reconstructed scale dependence of  $\beta$  show a similar behaviour as our model, where  $\beta$  from  $P_{\text{vg}}/P_{\text{gg}}$  declines with  $k$ , while that from  $(P_{\text{vv}}/P_{\text{gg}})^{1/2}$  increases with  $k$  (see their figure 4). We caution that this comparison is just illustrative, since the two methods of analysis differ in details (such as the use of plane-parallel approximation) and so cannot be directly compared.

We can also extract the cross-correlation coefficient  $r = P_{\text{vg}}/[P_{\text{vv}}P_{\text{gg}}]^{1/2}$  from this analysis. For normal galaxies it is close to unity for  $k < 0.1h\text{Mpc}^{-1}$  and rapidly declines above that. This means that the galaxy density and velocity divergence as reconstructed from this method become poorly correlated on small scales. Given this it is meaningless to combine the different estimates of  $\beta$  to enhance the statistical significance, since they do not measure the same parameter and the two fields are only poorly correlated on small scales.

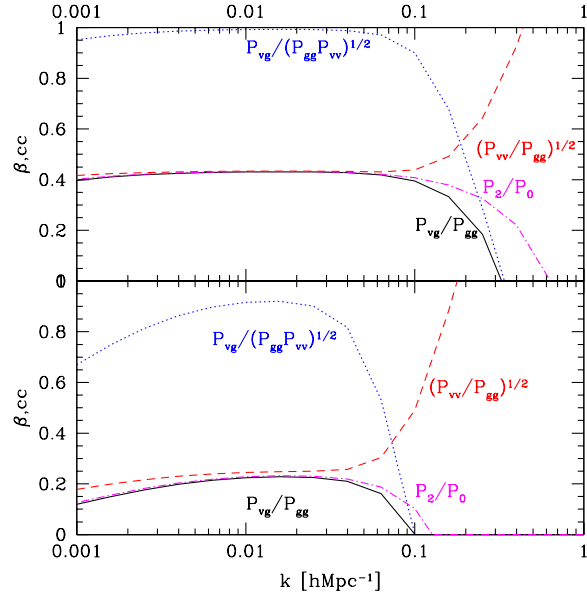


**Figure 2.** The predictions of the halo model for  $\beta$  using a variety of methods discussed in the text and galaxy-velocity cross-correlation coefficient. Top figure shows regular galaxies found also in the field, bottom shows biased (red, elliptical etc.) galaxies found predominantly in groups and clusters.

For biased (red or elliptical) galaxies found predominantly in groups or clusters the correlation is smaller than unity even on large scales and the agreement between different reconstructed  $\beta$  is less good there. This is mostly caused by the Poisson term, which is not negligible for galaxies on large scales. Divergence between  $\beta$  from different methods appears already for  $k \sim 0.04h\text{Mpc}^{-1}$ , caused by the more significant influence of massive halos with larger velocity dispersions. One should therefore be specially careful when drawing conclusions on cosmological parameters from this sample of galaxies, as for example from the planned bright red galaxy sample (BRG) in SDSS.

Another often used way to extract  $\beta$  is to determine the ratio of quadrupole to monopole terms (Kaiser 1987), which in terms of the above quantities is given by  $P_{qm} = 2.5(3P_2/P_0 - 1)$ . In linear theory one predicts it to be (Cole, Fischer & Weinberg 1994)

$$P_{qm} = \frac{1 + 2\beta/3 + \beta^2/5}{4\beta/3 + 4\beta^2/7}. \quad (24)$$

By solving the quadratic equation above one can determine  $\beta$  as a function of scale. This quantity is also shown in figure 2 and has a similar behaviour to  $\beta$  from  $P_{\text{vg}}/P_{\text{gg}}$  ratio, although the suppression on small scales is delayed relative to it.

## 4 CONCLUSIONS

We have analyzed the redshift distortion effects using the halo model, which has proven to be remarkably successful in explaining nonlinear real space power spectrum of both galaxies and dark matter (Ma & Fry 2000; Peacock & Smith

2000; Scoccimarro et al. 2000; Seljak 2000), as well as redshift space power spectrum of the dark matter (White 2000). We have shown that redshift space bias for regular galaxies is likely to be constant only for  $k < 0.1h\text{Mpc}^{-1}$ . Between  $0.1h\text{Mpc}^{-1} < k < 1h\text{Mpc}^{-1}$  the bias declines by 10-20% and rises again above that. This may be important for attempts to extract the value of cosmological parameters from such measurements (Tegmark, Zaldarriaga & Hamilton 2000), which typically assume nonlinear effects are negligible up to  $k \sim 0.2 - 0.3h\text{Mpc}^{-1}$ .

One parameter that is particularly sensitive to this effect is neutrino mass, which suppresses the power spectrum roughly in the same scale range where bias also becomes scale dependent. Since it has the same effect the two can be degenerate over the quasi-linear regime and this would complicate the attempts of accurately determining the neutrino mass from such galaxy clustering measurements. Figure 1 shows that the effect of neutrino mass begins to affect the power spectrum already on scales larger than where the bias is scale dependent. This is good news for the efforts to extract the neutrino mass, but the effect can only be measured if very large scale correlations can be accurately measured. These are limited by finite volume sampling variance, which can only be reduced by having a larger volume, so that the amplitude of correlations can be reliably determined for  $k \ll 0.1h\text{Mpc}^{-1}$ . If only the information around  $k \sim 0.1h\text{Mpc}^{-1}$  is used then one *cannot* separate the scale dependent bias effects from those of massive neutrinos. Current surveys such as PSCz still have large errors for  $k \ll 0.1h\text{Mpc}^{-1}$  and the new generation of surveys, such as SDSS and 2dF, combined with a more detailed modelling, will be needed to determine the neutrino mass from these measurements.

Galaxies found in rare systems such as groups and clusters suffer from another effect. For such galaxies the Poisson term can be so strong that it can exceed the linear correlation term not only on small scales, but also on very large scales. This effect is not present for dark matter, which is protected from it by causality and conservation of mass and momentum (Zeldovich 1970). Because of this the bias can rise again for  $k < 0.01h\text{Mpc}^{-1}$ . Since on such large scales this is a pure Poisson term with the slope exactly  $n = 0$  one can attempt to model it as a sum of two contributions and its amplitude can be estimated from the small scales. Equivalently, one can perform the correlation function analysis, where this term is not present on large scales.

Determination of parameter  $\beta$  shows similarly a convergence to a single value for  $k < 0.1h\text{Mpc}^{-1}$ , at least for normal galaxies where the Poisson term does not become important on very large scales. Around and above  $k \sim 0.1h\text{Mpc}^{-1}$   $\beta$  rapidly becomes scale dependent. The actual behaviour depends on the specific analysis and  $\beta$  can either grow or decline with scale. This is caused by the effect of virial motions, which counter the linear compression effect and are more important in more massive halos, which dominate the nonlinear clustering on large scales. The model reproduces well the scale dependence of  $\beta$  seen in the analysis of the real data (Hamilton et al. 2000). The cross-correlation coefficient between the galaxy and the velocity field divergence as obtained from the redshift space distortions is close to unity below  $k \sim 0.1h\text{Mpc}^{-1}$  and rapidly declines above that. Galaxies and velocities are significantly less well cor-

related than the dark matter and the galaxies in real space analysis, where the cross-correlation coefficient is unity at least up to  $k \sim 1h\text{Mpc}^{-1}$  (Seljak 2000). Our results are in broad agreement with other recent analysis of nonlinear bias and its effect on redshift space distortions and  $\beta$  (Hatton & Cole 1999; Berlind, Narayanan & Weinberg 2000). Together these results argue for a need of a more refined analysis of redshift distortions and redshift space power spectrum if the statistical power of existing and upcoming redshift space surveys is to be fully exploited. This is needed both to reduce the systematic effects and to extend the analysis to smaller scales. Since the halo approach used here reproduces well the results of N-body simulations and semi-analytic models it can serve as a useful framework within which one can extract the true underlying cosmological model from the data.

## ACKNOWLEDGMENTS

I acknowledge the support of NASA grant NAG5-8084. I thank SISSA, Trieste, for hospitality during my visit.

## REFERENCES

Benson, A. J., Baugh, C. M., Cole, S., Frenk, C. S., Lacey, C. G. 2000, MNRAS, 316, 107  
 Berlind, A. A., Narayanan, V. K., Weinberg, D. H. 2000, preprint [astro-ph/0008305]  
 Carlberg, R. G., Yee, H. K. C., Morris, S. L., Lin, H., Hall, P. B., Patton, D. R., Sawicki, M., Shepherd, C. W. 2000, preprint [astro-ph/0008201]  
 Cole, S., Fischer, K. B., Weinberg, D. H. 1994, MNRAS, 267, 785  
 Diaferio, A., Kauffmann, G., Colberg, G. M., White, S. D. M. 1999, MNRAS, 307, 537  
 Eisenstein, D. J., Hu, W., Tegmark, M. 1999, ApJ, 518, 2  
 Fukuda Y. et al. 1998, PRL 113, 273  
 Hamilton, A. J. S., Tegmark, M., Padmanabhan, N. 2000, preprint [astro-ph/0004334]  
 Hatton, S. J., Cole, S. 1999, preprint [astro-ph/9905186]  
 Hu, W., Eisenstein, D. J., Tegmark, M. 1998, PRL, 80 5255  
 Kaiser N., 1987, MNRAS, 227, 1  
 Kauffmann, G., Colberg, J. M., Diaferio, A., White, S. D. M. 1999, MNRAS, 303, 529; *ibid* 1999, MNRAS, 307, 529  
 Ma C.-P., Fry J.N., 2000, preprint [astro-ph/0001347]  
 Moore, B., Governato, F., Quinn, T., Stadel, J., Lake, G. 1998, ApJ, 499, L5  
 Navarro J., Frenk C.S., White S.D.M., 1996, ApJ, 462, 563  
 Peacock J.A., Dodds S.J., 1994, MNRAS, 267, 1020  
 Peacock J.A., Smith R.E., 2000, preprint [astro-ph/0005010]  
 Press W., Schechter P., 1974, ApJ, 187, 425  
 Saunders, W. et al. 2000, MNRAS, 317, 55  
 Scoccimarro, R., Sheth, R. K., Hui, L., Jain, B. 2000, preprint [astro-ph/0006319]  
 Seljak U., 2000, preprint [astro-ph/0001493]  
 Sheth R., Tormen G., 1999, MNRAS, 308, 119 (1999)  
 Strauss, M. A., Willick, J. A. 1995, PhR, 261, 271  
 Tegmark, M., Zaldarriaga, M., Hamilton, A. J. S. 2000, preprint [astro-ph/0008167]  
 White M. 2000, preprint [astro-ph/0005085]  
 Zeldovich Y. 1970, A & A, 5, 84